Published in final edited form as:
Anticancer Agents Med Chem. 2011 February ; 11(2): 202–212.

Cellular Redox Modulator, *ortho* Mn(III) *meso*-tetrakis(*N*-n-Hexylpyridinium-2-yl)porphyrin, MnTnHex-2-PyP^{5+} in the Treatment of Brain Tumors

Stephen T. Keir[1,2,*], **Mark W. Dewhirst**[3], **John P. Kirkpatrick**[3], **Darell D. Bigner**[1,4], and **Ines Batinic-Haberle**[3,*]

[1]The Preston Robert Tisch Brain Tumor Center at Duke, Duke University, Durham NC, 27710, USA

[2]Department of Surgery, Duke University, Durham NC, 27710, USA

[3]Department of Radiation Oncology, Duke University, Durham NC, 27710, USA

[4]Department of Pathology, Duke University, Durham NC, 27710, USA

Abstract

Despite intensive efforts to improve multimodal treatment of brain tumors, survival remains limited. Current therapy consists of a combination of surgery, irradiation and chemotherapy with predisposition to long-term complications. Identifying novel targeted therapies is therefore at the forefront of brain tumor research. This study explores the utility of a manganese porphyrin in a brain tumor model. The compound used is *ortho* isomer, manganese(III) *meso*-tetrakis(*N*-n-hexylpyridinium-2-yl)porphyrin, MnTnHex-2-PyP^{5+}. It is a powerful SOD mimic and peroxynitrite scavenger and a potent modulator of redox-based cellular transcriptional activity, able to suppress excessive immune and inflammatory responses and in turn proliferative pathways. It is further one of the most lipophilic compounds among cationic Mn(III) *N*-alkylpyridylporphyrins, and thus accumulates predominantly in mitochondria relative to cytosol. In mitochondria, MnTnHex-2-PyP^{5+} could mimic our key antioxidant system, mitochondrial superoxide dismutase, MnSOD, whose overexpression has been widely shown to suppress tumor growth. Importantly, MnTnHex-2-PyP^{5+} crosses blood brain barrier in sufficient amounts to demonstrate efficacy in treating CNS injuries. For those reasons we elected to test its effects in inhibiting brain tumor growth. This study is the first report of the antitumor properties of MnTnHex-2-PyP^{5+} as a single agent in adult and pediatric glioblastoma multiforme (D-54 MG, D-245 MG, D-256 MG, D-456 MG) and pediatric medulloblastoma (D-341 MED), and is the first case where a redox-able metal complex has been used in glioma therapy. When given subcutaneously to mice bearing subcutaneous and intracranial xenografts, MnTnHex-2-PyP^{5+} caused a significant ($P \leq 0.001$) growth delay in D-245 MG, D-256 MG, D-341 MED, and D-456 MG tumors. Growth delay for mice bearing subcutaneous xenografts ranged from 3 days in D-54 MG to 34 days in D-341 MED. With mice bearing intracranial xenografts, MnTnHex-2-PyP^{5+} increases median survival by 33% in adult glioblastoma multiforme (D-256 MG; $P \leq 0.001$) and 173% in pediatric medulloblastoma (D-341 MED, ≤0.001). The beneficial effects of MnTnHex-2-PyP^{5+} are presumably achieved either (1) indirectly *via* elimination of signaling reactive oxygen and nitrogen species (in particular superoxide and peroxynitrite) which in turn would prevent

*Address correspondence to these authors at the Preston Robert Tisch Brain Tumor Center, Department of Surgery, Duke University Medical Center, Box 3624 DUMC, Durham, North Carolina 27710 USA; Tel: 919-684-2317; Fax: 919 684-8203; Keir0001@mc.duke.edu; and at the Department of Radiation Oncology-Cancer Biology, Duke University Medical Center, Research Drive, 281b/285 MSRB I, Box 3455, Durham, NC 27710, USA; Tel: 919-684-2101; Fax: 919-684-8718; ibatinic@duke.edu.

activation of transcription factors; or (2) directly by coupling with cellular reductants and redox-sensitive signaling proteins. The former action is antioxidative while the latter action is presumably pro-oxidative in nature. Our findings suggest that the use of Mn porphyrin-based SOD mimics, and in particular lipophilic analogues such as MnTnHex-2-PyP^{5+}, is a promising approach for brain tumor therapy.

Keywords

Brain tumors; glioma; porphyrins; novel anticancer therapeutic strategy; SOD mimic; peroxynitrite scavenger; MnTnHex-2-PyP^{5+}

INTRODUCTION

Brain Tumors

Glioblastoma is the most frequent and aggressive primary brain tumor in adults, and despite surgical resection and chemoradiotherapy followed by adjuvant temozolomide, its prognosis remains poor, with a median survival of approximately 15 months [1, 2]. Almost all patients ultimately develop progressive tumors after initial treatment, with median survival following recurrence of only about 6 months [3, 4]. Medulloblastoma is the most common brain tumor in children [1]. Treatment for this disease includes surgery, craniospinal irradiation, and chemotherapy. The 5-year progression-free survival of medulloblastoma patients ranges from 40% to 70%, and most survivors experience a combination of long-term, treatment-related neurocognitive deficits [5, 6]. Due to the typically poor outcomes for patients with brain tumors, novel therapeutic strategies and agents are desperately needed.

Porphyrins in Tumor Therapy

Various investigators have developed diagnostic or therapeutic drugs for cancer using porphyrin derivatives. The aim of most of those studies was to refine current methods for photodynamic therapy [7]. Over the last 20 years, more than 1,200 types of porphyrin derivatives have been synthesized. Modifications of their structures, affinities for tumor tissues, and mechanisms of action have been studied with the ultimate goal to develop them for use in cancer diagnosis and treatment [8–15]. The mechanism of photodynamic therapy is a pro-oxidative one, where killing occurs *via* enhanced production of reactive species.

Mn(III) *N*-Alkylpyridylporphyrins

Cationic manganese (III) *ortho N*-ethylpyridylporphyrin, MnTE-2-PyP^{5+} (AEOL10113), and related *ortho* analogues, such as Mn(III) *meso*-tetrakis(*N*-n-hexylpyridinium-2-yl)porphyrin, MnTnHex-2-PyP^{5+} (Fig. **1**) and Mn(III) *meso*-tetrakis(*N,N'*-diethylimidazolium-2-yl)porphyrin, MnTDE-2-ImP^{5+} (AEOL10150) are among the most potent catalytic scavengers of superoxide, $O_2^{\cdot -}$ and peroxynitrite, $ONOO^-$ [16, 17]. MnTE-2-PyP^{5+} was the first developed and thus mostly studied *in vivo* [16–18]. Their potency depends on the presence of cationic charges on pyridyl nitrogens in *ortho* positions (Fig. **1**). Such placement close to the metal site exerts an electron-withdrawing effect and consequently affords a favorable reducibility of manganese [16–18]. In addition such position of charges affords electrostatic attraction for the incoming anionic superoxide and peroxynitrite [16–18]. The action of Mn porphyrins (MnPs) in scavenging $O_2^{\cdot -}$ and $ONOO^-$ is likely coupled with cellular reductants, due to their high cellular levels [16, 17]. Such coupling, while supporting their antioxidative action/s, may be involved in their pro-oxidative action/s also; see Discussion. Cationic Mn(III) *N*-substituted pyridylporphyrins, and in particular *ortho* isomers posses properties that allow them to inhibit activation of major transcription factors as shown with MnTE-2-PyP^{5+} for HIF-1α, AP-1 and NF-κB,

with MnTDE-2-ImP^{5+} for HIF-1α, SP-1 and NF-κB and with MnTnHex-2-PyP^{5+} for HIF-1α and NF-κB [16–23]. Consequently, these compounds suppress excessive inflammatory and immune responses in numerous animal models of diseases [16–18]. The specificity of the effects of MnPs on cellular transcription activity may arise from the different redox status of tumor *vs* normal cells. It may also be due to the different transcription factor profile in tumor *vs* non-tumor cells.

The therapeutic effects of cationic Mn(III) porphyrins as well as their chemistry and biology have been recently reviewed in detail [16–18]. A number of reports have demonstrated their therapeutic potential in cancer therapy when given either alone or combined with radiation, heat and chemotherapy [16–18]. Examples include studies with the 4T1 mouse breast tumor [21–23, Jackson *et al.* unpublished], mouse skin carcinogenesis [24], lymphoma [25, 26] and a mouse prostate tumor model [27] (see Discussion for details).

A more lipophilic analogue with antioxidant potency equal to that of MnTE-2-PyP^{5+}, Mn(III) *ortho N*-n-hexylpyridylporphyrin, MnTnHex-2-PyP^{5+} (Fig. **1**, Table **1**), was developed recently [16– 18]. With this compound we aimed primarily at increasing MnP accumulation within the cell and particularly in critical cellular compartments mitochondria (see below), and enhancing its ability to cross the blood brain barrier (BBB). MnTnHex-2-PyP^{5+} is 13,500-fold more lipophilic than its ethyl analogue, MnTE-2-PyP^{5+} (Table **1**) [28]. The difference in lipophilicity between MnTnHex-2-PyP^{5+} and MnTE-2-PyP^{5+} (Table **1**) translates to up to 2 orders of magnitude difference in their *in vivo* efficacy [16–18]. Of particular relevance to brain tumors, lipophilic hexyl porphyrin, MnTnHex-2-PyP^{5+} reaches brain at higher levels compared to the hydrophilic ethyl analog, MnTE-2-PyP^{5+} [29, 30]. In a recent mouse pharmacokinetic study, MnTnHex-2-PyP^{5+} levels in brain at 24 hours were 8-fold higher relative to MnTE-2-PyP^{5+} [29]. These two Mn porphyrins differ also with respect to the ease of their reduction from Mn^{III}P^{5+} to Mn^{II}P^{4+} (Table **1**). MnTnHex-2-PyP^{5+} is more readily reducible than MnTE-2-PyP^{5+}, which would favor its coupling with cellular reductants while removing reactive species (Table **1**). Finally, they differ with respect to the shape, size of the molecule, steric hindrance of cationic charges, which may also affect their differential *in vivo* efficacy [16–18]. MnTnHex-2-PyP^{5+} is bulkier than MnTE-2-PyP^{5+} which may outbalance to some extent the favorable effect of its lipophilicity on the transport across cellular membranes and the BBB. In a 4T1 mouse breast cancer study, MnTnHex-2-PyP^{5+} was found to favor tumor accumulation 5-fold more than a muscle [31]. Thus far, MnTnHex-2-PyP^{5+} has been efficient in all *in vitro* and *in vivo* models of oxidative stress studied, while the more hydrophilic MnTE-2-PyP^{5+} failed in two studies: radioprotection of ataxia telangiectasia [32], and a rabbit cerebral palsy model [33, Drobyshevsky *et al.* unpublished]. The failure was ascribed to the inability of MnTE-2-PyP^{5+} to accumulate in mitochondria and cross the BBB at pharmacologically effective levels.

Mitochondria, the highly dynamic organelles, are crucial for the life and death of the cells. They have been linked to apoptosis, maintenance of cellular homeostasis, and ultimately to neurologic disorders and metabolic diseases. Therefore therapeutic strategies targeting mitochondria have been actively sought (see Discussion). Lipophilic, positively charged compounds accumulate in mitochondria driven there by the mitochondrial membrane potential [34, 35]. Accordingly, MnTnHex-2-PyP^{5+} accumulates in yeast mitochondria at >90% relative to cytosol, and more than hydrophilic MnTE-2-PyP^{5+}, mimicking there superoxide dismutase [36]. While an earlier mouse study showed that MnTE-2-PyP^{5+} accumulated in heart mitochondria at levels high enough to protect it against peroxynitrite-mediate damage [37], we have not looked at its cytosolic levels. In a subsequent mouse heart mitochondria study, similar to yeast, MnTnHex-2-PyP^{5+} was found predominantly in mitochondria relative to cytosol [Spasojevic *et al.* in preparation]. We ascribe the

remarkable potency of both compounds in *in vivo* models of oxidative stress at least in part to their mitochondrial accumulation where they can mimic MnSOD. The skin carcinogenesis study, where timely administration of MnTE-2-PyP^{5+} produced effects similar to those produced when MnSOD was overexpressed, suggests that MnP accumulates in mitochondrial matrix [24]. For final proof of the accumulation site within mitochondria, further work is needed to analyze inner and outer mitochondrial membranes as well as intermembrane space on MnP levels. Mitochondrial superoxide dismutase, MnSOD, is an essential antioxidant defense against excessive superoxide produced during respiration and generation of ATP. It has been widely substantiated that MnSOD overexpression suppresses tumor growth [reviewed in 38, in this issue].

In summary, we have chosen to assess the therapeutic efficacy of MnTnHex-2-PyP^{5+} in treating human brain tumors in a mouse model for several reasons: (1) it is among the most potent SOD mimics and peroxynitrite scavengers; (2) it is a potent modulator of redox-based cellular transcriptional activity; (3) it accumulates in tumor relative to normal tissue; (4) it is among the most lipophilic cationic Mn porphyrins, and thus: (a) accumulates predominantly in mitochondria relative to cytosol where it could mimic mitochondrial superoxide dismutase, MnSOD, and (b) crosses the BBB.

MATERIALS AND METHODS

Animals

Female athymic mice (nu/nu genotype, Balb/c background, 6 to 8 weeks old) were used for all antitumor studies. Animals were maintained in filter top cages in Thoren units (Thoren Caging Systems, Inc., Hazelton, PA). All animal procedures conformed to Institutional Animal Care and Use Committee and National Institute of Health guidelines.

Tumor Xenografts and Implantation

The following patient-derived human tumor xenografts maintained at the Preston Robert Tisch Brain Tumor Center at Duke were used both for intracranial (ic) and subcutaneous (sc) studies: D-341 MED, a pediatric medulloblastoma and three adult glioblastoma multiforme xenografts: D-54 MG, D-245 MG, and D-256 MG. D-456 MG was also screened as a part of this study, but was only implanted subcutaneously.

For intracranial studies, subcutaneous xenografts passaged in athymic mice were excised from host mice under sterile conditions in a laminar flow containment hood. The entire tumor was resected from the host animal, and necrotic tissue visible to the eye was removed. The xenograft was minced and cells separated with a 60 mesh tissue cytosieve (Biowhitter Inc, Walkersville, MD) into a Zinc Option solution, allowing for passage through a 25 gauge needle. After centrifugation, supernatant was removed, and cells were mixed 1:1 with methylcellulose. This mixture was then loaded into a repeating 250-/J Hamilton syringe (Hamilton, Co., Reno, NV) dispenser and injected ic into the right cerebral hemisphere of the athymic mouse at an inoculation volume of 10 μl. The ic injections were done by placing a mouse into a stereotactic frame. A 1/2” midline skin incision was made. The bregma was located and the coordinates (2 mm lateral) determined. A mounting holder on the frame holds the syringe containing the cells. A sterile 25 gauge needle attached to the syringe was introduced through the calvaria and into the brain at a depth of 4 mm. The cells were injected and after one minute, the syringe was pulled up and a small amount of bone wax was placed to occlude the hole. The mouse was removed from the frame and wound clips were used to close the skin [39–42]. All mice, control and treated, were injected with the same volume of tumor homogenate, assuring the same number of tumor cells injected into each mouse.

In preparation for sc transplantation, tumors were prepared as indicated above and placed into a modified tissue press. The resulting homogenate was then loaded into a repeating Hamilton syringe dispenser. Tumor homogenate was injected sc into the right flank of the athymic mouse at an inoculation volume of 50 μl with a 19 gauge needle [39]. Due to sterile technique, no infection was observed. Lidocaine and Bupivicaine were used to control the pain.

Subcutaneous Tumor Measurement

Subcutaneous tumors were measured twice weekly with handheld vernier calipers (Scientific Products, McGraw, IL). Tumor volumes, V were calculated with the following formula: $[\text{width}^2 \times \text{length}]/2 = V\ (\text{mm}^3)$.

Subcutaneous and Intracranial Xenograft Therapy with MnTnHex-2-PyP^{5+}

For the sc tumor studies, groups of mice randomly selected by tumor volume were treated when the median tumor volumes were on average 250 mm^3 and were compared with control animals receiving vehicle (saline). For ic tumor studies, groups of mice were randomized 3 days after ic tumor implantation [43]. MnTnHex-2-PyP^{5+} was injected sc at a dose of 1.6 mg/kg b.i.d. throughout the duration of the experiment. The volumes were adjusted to the weight of the mice and were 300 μL on average. At dose used no adverse effects on mouse overall health were observed (see below under Toxicity of MnP).

Mn Porphyrin Synthesis

MnTnHex-2-PyP^{5+} was prepared as previously described [16, 17]. Briefly, 11 mL of n-hexyl *p*-toluenesulfonate was added to a mixture of 75 mg of H_2T-2-PyP (Frontier Scientific) in 20 mL *N,N'*-dimethylformamide and heated at ~100°C. Reaction was followed by thin-layer chromatography (TLC) on silica gel TLC plates using 8:1:1 = acetonitrile:$KNO_{3(sat)}$:H_2O as a mobile phase. Completion was indicated by the lack of any change in two consecutive TLC runs. Upon completion, the reaction mixture was poured in a separatory funnel containing 200 mL each of water and chloroform and shaken well. Tetracationic porphyrin has tosylates as counterions, and is thus fairly lipophilic. Further, the excess of DMF and tosylate keeps it also from distributing readily into aqueous layer. Thus porphyrin tends first to form a third layer. Several extractions are needed to remove the excess DMF and tosylate. The dropwise addition of methanol to the mixture is often helpful to push porphyrin into aqueous layer. When the extraction was completed, the aqueous layer was filtered into glass bealker where porphyrin was precipitated as PF_6^- salt by dropwise addition of a concentrated aqueous solution of NH_4PF_6 until no further precipitate was formed. Precipitate was filtrated through a fritted disc and thoroughly washed on a disc with diethyl ether. Dried precipitate was dissolved in acetone and filtered. The porphyrin was precipitated out of acetone solution as a chloride salt with dropwise addition of saturated acetone solution of tetrabutylammonium chloride [17]. The precipitate was washed thoroughly with acetone (to remove any traces of tetrabutylammonium chloride, which is toxic to cells and animals) and dried in vacuum at room temperature. When the ligand was used only to prepare Mn complex and not for other purposes, single precipitation was sufficient.

For metallation, 20-fold excess $MnCl_2$ was added to a pH ~10.7 solution of porphyrin at 25 °C to ensure the presence of both kinetically more reactive Mn(II) monohydroxoaqua species, and deprotonated inner pyrrolic nitrogens of porphyrin [17]. With a longer alky-chain analogue such as hexyl porphyrin, the heating of a solution for hours at ~100°C is often needed. The reaction progress was followed by uv/vis spectroscopy and TLC (8:1:1 = acetonitrile: $KNO_{3(sat)}$:H_2O) until the disappearance of the Soret band and fluorescence of the metal-free porphyrin. Porphyrin is stable under such conditions and it is not critical to

stop the metallation at the exact moment of completion. Upon completion, the solution was filtered to remove the excess of free Mn in the form of Mn oxo/hydroxo species. The porphyrin was precipitated as PF_6^- salt from filtrate by dropwise addition of saturated aqueous solution of NH_4PF_6 and washed with diethyl ether. Precipitate was dissolved in acetone, and the porphyrin chloride salt was precipitated with saturated acetone solution of tetrabuthylammonium chloride, and the resulting precipitate was washed with acetone. The $PF^-_{6\ (aq)}/Cl^-_{(acetone)}$ precipitation procedure was repeated twice to ensure the full removal of free manganese. A chloride salt, MnTnHex-2-PyPCl_5 was utilized in this study. Its identity and purity was checked by uv/vis spectroscopy, elemental analysis, thin-layer chromatography, electrospray mass spectrometry and the analysis of free Mn (lowmolecular weight Mn complexes) [17].

Evaluation of Subcutaneous Xenograft Response to MnP Treatment

The response of sc xenografts to MnP treatment was assessed by delay in tumor growth and by tumor regression. Growth delay, expressed as T-C, is defined as the difference in days between the median time required for tumors in treated (T) and control (C) animals to reach a volume five times greater than that measured at the start of the treatment. Tumor regression is defined as a decrease in tumor volume over two successive measurements. Statistical analysis was performed using a SAS statistical analysis program, the Wilcoxon rank order test for growth delay, and Fisher's exact test for tumor regression as previously described [39, 44].

Evaluation of Intracranial Xenograft Response to MnP Treatment

The response of ic xenografts to MnP treatment was assessed by percentage increase in time to a specific neurologic endpoint (seizure activity, repetitive circling, or other subtle changes such as grooming or decrease in appetite) or to death. Statistical analysis was performed using the Wilcoxon rank order test as previously described [39, 44]. Animals were observed twice daily for signs of distress or development of neurologic symptoms, at which time, the mice were sacrificed.

RESULTS

Toxicity of MnP

A preliminary toxicity study was conducted in mice bearing D-245 MG ic tumors to determine the appropriate dosage for all subsequent studies. Doses of MnTnHex-2-PyP^{5+} tested were in the range of 0.1 mg/kg to 1.6 mg/kg given sc b.i.d. (twice daily) for the duration of the experiment (Fig. **2**). Control animals received an equal volume of saline. Previous studies have used doses of MnP ranging from 0.05 to 2 mg/kg/day given *via* different routes of administration [16, 17].

Among the 115 mice treated, no deaths were attributed to drug toxicity. The median nadir weight loss for treated animals was 3.2%. No neurologic toxicity of MnP was observed. No significant dose response was detected in the range of doses studied. Given the doses used elsewhere, and the lack of the toxicity of MnP at 3.2 mg/kg/day we have chosen to use this dose for efficacy studies.

Efficacy

Subcutaneous Xenograft Therapy by MnP—MnTnHex-2-PyP^{5+} produced statistically significant ($P \leq 0.001$) growth delays in D-245 MG, D-256 MG, D-341 MED, and D-456 MG (Table **2**) xenografts. Growth delays ranged from 3 days in D-54 MG to 34

days in D-341 MED. Tumor regression was seen in studies with D-245 MG, D-341 MED, and D-456 MG. Control animals received an equal volume of saline.

Intracranial Xenograft Therapy by MnP—MnTnHex-2-PyP^{5+} produced a statistically significant ($P \leq 0.001$) increase in median survival in D-256 MG and D-341 MED of 33% and 171%, respectively (Table **3** and Figs. **3** and **4**). All mice displayed gross evidence of ic tumors at the time of death.

In both subcutaneous and intracranial xenografts the suppression of tumor growth was larger with pediatric tumors than with adult glioblastomas.

DISCUSSION

Cationic Mn(III) *N*-alkylpyridylporphyrins that have metal-centered reduction potential for Mn^{III}P^{5+}/Mn^{II}P^{4+} redox couple between ~+50 and~+500 mV *vs* NHE can easily adopt 4 oxidation states *in vivo* (+2, +3, +4, and +5), which allows them to undergo a variety of redox-based reactions with reactive oxygen and nitrogen species, cellular reductants and signaling molecules (in particular with cysteines of those proteins which may be oxidized or glutathionylated; both modifications have been reported (Fig. **1**) [16–18, 26]. They are the most potent SOD mimics and ONOO^{-} scavengers reported (Fig. **1**) [16–18]. Cell biology is greatly redox-based. Thus it is only natural that very redox-able compounds could finely tune cellular apoptotic and proliferative pathways *via* modulation of redox-based transcriptional activity (Fig. **1**), which would in turn lead to modulation of inflammatory and immune responses [16–18]. Recent data indicate that cationic Mn porphyrins can differentiate between tumor and normal tissue [31]. MnTnHex-2-PyP^{5+} accumulates 5-fold more in 4T1 tumors than in muscle taken from the opposite leg (Fig. **1**) [31]. Favoring tumor over normal tissue may arise in part from the differential redox status of such tissues and in particular from their differential ability to remove superoxide and peroxides [45–48]. Higher tumor oxidative stress would result in compromised cellular and mitochondrial membranes which may contribute to leaky tumor vasculature. Another reason may be the higher surface area of cancer cells due to the higher number of microvilli and thus more chances to interact with a drug. Finally, cancer cells have a net negative surface charge due to the higher expression of anionic molecules, such as phosphatidylserine, O-glycosylated mucins, sialilated gangliosides and heparin sulfates [49–55]. These negatively charged molecules facilitate interaction and penetration of the cationic species through the membrane.

While maintaining the high redox-ability, we modified the structure of Mn porphyrins to increase their bioavailability. Primarily, compounds with increased lipophilicity, and thus cellular, subcellular (particularly mitochondrial) and tumor accumulation as well as those able to cross the BBB were synthesized (Fig. **1**). Such efforts have been aimed at more promising drugs for CNS injuries including brain tumors. Thus far, the most prospective has been a lipophilic MnTnHex-2-PyP^{5+} (Fig. **1**). This study is the first and encouraging report of the antitumor properties of a metal complex, MnTnHex-2-PyP^{5+} as a single agent in adult and pediatric glioblastoma multiforme and pediatric medulloblastoma. Tumor growth was significantly inhibited by MnTnHex-2-PyP^{5+} in 4 out of the 5 brain tumor lines (Figs. **2**, **3** and **4**). When given subcutaneously to mice, MnTnHex-2-PyP^{5+} caused a significant ($P \leq 0.001$) growth delay in D-245 MG, D-256 MG, D-341 MED, and D-456 MG xenografts. Growth delay for mice bearing subcutaneous xenografts ranged from 3 days in D-54 MG to 34 days in D-341 MG. With mice bearing intracranial xenografts, MnTnHex-2-PyP^{5+} produced a statistically significant ($P \leq 0.001$) increase in median survival of the mice for 33% (D-256 MG) and 173% (D-341 MED).

Our data on both subcutaneous and intracranial xenografts indicate a better response of pediatric than adult tumors (Tables **2** and **3**). In general, pediatric medulloblastomas are more sensitive to adjuvant irradiation and chemotherapy than malignant gliomas [56], which is in agreement with this study. Given the limited number of tumors evaluated in this study (3 adult malignant gliomas, 1 pediatric glioma and 1 pediatric medulloblastoma in 2 different sets of experiments) we cannot speculate further about the nature of the differential response of these tumors to MnP treatment.

With the exception of completely resected low-grade glioma, radiation therapy remains a component of therapy care for most patients. However, most children exposed to radiation therapy have significant neurocognitive and endocrinologic sequelae and significant late effects [57]. Thus, there is a need for therapeutic approaches to reduce the toxicity of radiotherapy or eliminate the need for it [58]. In search for new therapies, different pathways have been explored with medulloblastomas (such as Hedgehog, Wnt and Notch) [59] and with gliomas (receptor tyrosine kinases, Src family of non-receptor protein kinases, intracellular signaling molecules such as EGFR-PI3K-Akt-mTOR signaling network [60], epigenetic abnormalities, tumor vasculature, microenvironment stem cells, mitochondria etc [61, 62]). As glioblastoma multiforme is almost invariably fatal, any breakthrough may have a substantial impact on survival and provide hope to the thousands of patients who receive this diagnosis annually [63].

In addition to suppressing tumor growth, MnTnHex-2-PyP^{5+} and other analogues reportedly possess remarkable ability to radioprotect normal tissue [16–18]. MnPs produce radioprotective effects in animal studies of lung, brain, eye, prostate, colon, and hematopoietic cells [16–19, 20, 32, 64–69, Archambeau *et al.* unpublished], and zebra fish embryo [16, 17, Daroczi *et al.*, unpublished]. The most extensively studied organ has been lung [19, 20, 64]. When the methyl analogue, MnTM-2-PyP^{5+} was administered for 2 weeks prior to 8 Gy whole body radiation, 80% of the radiated mice survived relative to the control counterparts [70]. The post total body treatment (TBI) with NADP oxidase inhibitor diphenylene iodonium or MnTE-2-PyP^{5+} not only significantly reduced TBIinduced increases in reactive oxygen species production, oxidative DNA damage and DNA double-strand breaks in hematopoietic stem cells (HSC), but also dramatically decreasesd the number of cells with unstable chromosomal aberrations in the clonal progeny of irradiated HSCs [65, 68]. Recent studies reported that MnTE-2-PyP^{5+} treatment prior to brain irradiation protected against acute radiation-induced apoptosis and ameliorated delayed damage to the blood-brain barrier and radiation necrosis [66]. Finally, MnTE-2-PyP^{5+} altered cytokine responses after irradiation in a prostate tumor model and shows a potential to enhance anti-tumor immune responsiveness and decrease the risk for radiation-induced normal tissue toxicities [67]. Consequently, the use of Mn porphyrins could enhance the therapeutic margin by sensitizing the tumor and protecting normal tissue at the same time.

Mechanistic Considerations

This study aimed primarily to show if there is a therapeutic potential of a novel strategy in employing a metal complex in treating brain tumors. The use of a metal complex is still a rarity in clinics. It has been known for nearly 50 years that tumors exist under conditions of perturbed redox status which results in oxidative stress with increased levels of reactive species [71]. The excessive reactive species drive the tumor growth; they originate from dysfunctional cells; most so from mitochondrial respiratory chain and hypoxic conditions (in particular conditions of hypoxia/reoxygenation occurring during tumor growth). Further, the upregulation of NADPH oxidase and inducible nitric oxide synthase contribute to the production of $O_2^{\cdot -}$, $^{\cdot}NO$, $ONOO^-$ and their progeny [72–80, 81]. The predominant function of MnTnHex-2-PyP^{5+} in the case of tumors is likely the redox-based suppression of

oxidative stress *via* modulation of redox-sensitive cellular pathways which control tumor proliferation and apoptosis [16–18]. This modulation may be indirect by removing reactive species that would otherwise activate transcription factors (antioxidative mechanism), or direct by oxidizing transcription factors such as NF-κB (pro-oxidative mechanism) [18, 26, 82].

During the two-step $O_2^{\cdot -}$ dismutation process, the MnP is oxidizing $O_2^{\cdot -}$ (producing O_2) in one half-, and reducing $O_2^{\cdot -}$ (producing H_2O_2) in another half-reaction. With enzymes and with the most potent MnPs, such as MnTE-2-PyP^{5+} and MnTnHex-2-PyP^{5+}, both processes, oxidation and reduction of $O_2^{\cdot -}$, occur with the similar rate constants [16, 17, 83]. Such fact clearly suggests that Mn porphyrins could act both as anti- and pro-oxidants in an *in vivo* setting. Future efforts are directed towards understanding which mechanism of MnP action, and under what conditions, prevails *in vivo*.

Antioxidative Mechanism of *In Vivo* MnP Action/s

The antioxidative type of action has been supported by experimental evidences in numerous reports which are summarized in refs 16 and 17, and briefly herein. Our previous mouse 4T1 breast cancer studies indicate that Mn porphyrin, MnTE-2-PyP^{5+} inhibits HIF-1α and therefore downregulates VEGF and bFGF expression which in turn inhibits tumor angiogenesis and sensitizes tumor microvasculature and tumor cells to radiation [21–23]. The suppression of oxidative stress was reported also [21]. The proposed antioxidative mechanism was the removal of signaling species that would have otherwise activated HIF-1α. MnTE-2-PyP^{5+} was further tested in a well-established mouse skin carcinogenesis model which consists of sequential application of a subthreshold dose of the mutagenic chemical initiator 7,12-dimethylbenz(*a*)-anthracene (DMBA), followed by repetitive treatments with the tumor promoter 12-*O*-tetradecanoylphorbol-13-acetate (TPA). In this model, MnTE-2-PyP^{5+} markedly suppressed both tumor incidence and multiplicity: in groups consisting of 11 animals, 30 papillomas developed in the control group *vs* 5 in the MnP-treated group [24]. Further, MnTE-2-PyP^{5+} strongly suppressed the activation of AP-1 transcription factor which controls cellular proliferation. Consequently, proliferating cellular nuclear antigen, PCNA was down-regulated [24]. The anticancer effects were greatly enhanced when MnTE-2-PyP^{5+} was combined with radiation in a 4T1 breast cancer mouse model [22, 23]. Also the Balb/c nu/nu mouse study in progress on D-245 MG sc xenografts, where MnTnHex-2-PyP^{5+} is combined with radiation, shows the greatly enhanced suppression of tumor growth relative to either treatment alone [Rajic *et al.* unpublished]. Remarkable suppression of B16F10 melanoma growth was observed in C57/BL6 mice when MnTE-2-PyP^{5+} was combined with hyperthermia [Jackson *et al.* unpublished]. In a mouse prostate cancer tumor model RM-9, the combined treatment of MnTE-2-PyP^{5+} with radiation slowed the growth of tumors, provided benefit over radiation alone, enhanced immune response, increased number of natural killer cells, and ability to produce IL-2 [27].

Pro-Oxidative Mechanism of In Vivo MnP Action/s

Such action/s is facilitated by the high intracellular levels (mM) of cellular reductants such as ascorbate [84], glutathione and the bioavailability of oxygen. In particular the coupling of MnP with ascorbate (Fig. **1**) may be relevant to gliomas, because the brain and spleen are the organs with the highest levels of ascorbate [85, 86]. The pro-oxidative action may occur when porphyrins are given either alone or with exogenous ascorbate. In a pro-oxidative scenario [87], $Mn^{III}P^{5+}$ gets readily reduced to $Mn^{II}P^{4+}$ with ascorbate in a first step of a dismutation process. In a subsequent step, the reduced $Mn^{II}P$ may reduce oxygen (rather than superoxide) to $O_2^{\cdot -}$ which would then readily dismute to cytotoxic H_2O_2. Also, MnP catalyzes the oxidation of ascorbate to the ascorbyl radical in a first step (while being reduced to $Mn^{II}P$) [47, 88]. The ascorbyl radical would undergo oxidation to

dehydroascorbate in a subsequent step, while reducing oxygen to superoxide; eventually H_2O_2 would be formed [87]. In either scenario, peroxide would either kill the tumor in its own right *via* causing oxidative damage to biological targets, or act as a signal for upregulation of cellular transcriptional activity which may perpetuate oxidative stress forcing cells to die eventually. H_2O_2 can also inflict toxicity *via* producing highly damaging species, $^{\cdot}OH$ radical, in a Fenton-type reaction with Fe^{2+} [89, 90]. The tumors are already under oxidative stress [91], and are very sensitive to any additional increase in oxidative burden which could signal cell death [26, 87].

Several reports support the pro-oxidative action of Mn porphyrins. When combined with chemotherapy, MnTE-2-PyP^{5+} sensitized WEHI7.2 murine thymic lymphoma cells to cyclophosphamide and inhibited cell growth, at least in part *via* pro-oxidative mode of action inhibiting activation of NF-κB *via* glutathionylation of its p65 subunit [25, 26]. A modified porphyrin of extended core, Gd(III) texaphyrin (Motexafin gadolinium, MGd, Xcytrin [Pharmacyclics, Sunnyvale, CA]), combined with radiation has been used with varying success for the treatment of brain metastases [92, 93]. MGd kills tumor cells presumably *via* increased production of reactive species, that is, *via* a pro-oxidative mode of action, similar to photodynamic therapy; only the source of reactive species is different. In another, amyotrophic lateral sclerosis study, both MGd and MnTnHex-2-PyP^{5+} [94] were compared to each other and produced similar effects, although an antioxidative mode of action was proposed for the latter and a pro-oxidative for the former. The data suggest that perhaps both MGd and MnTnHex-2-PyP^{5+}, may act *via* common, pro-oxidative action. In our most recent study, 4 different cancer cell lines were treated with MnTnHex-2-PyP^{5+} alone and in combination with ascorbate [95]. Data clearly indicate that remarkable cancer cell killing with MnP + ascorbate treatment was achieved *via* pro-oxidative action where Mn porphyrin acts as catalyst for ascorbate-driven peroxide formation [95]. Recently, in cellular and *in vivo* ip and iv studies it was clearly pointed to the antitumor potential of ascorbate where peroxide production was catalyzed by redox-able compounds, such as quinones and endogenous porphyrins [84, 86, 96–99]. We have recently explored a simple straightforward superoxide-specific system – aerobic growth of SOD-deficient *E. coli* [87]. Without SOD mimic, this strain grows poorly under aerobic conditions in a nutrient-poor medium, but grows as good as wild type in the presence of Mn porphyrin-based SOD mimics. If the medium contains both Mn porphyrin and ascorbate the SOD-deficient *E. coli* does not grow; the effect is reversed in the presence of catalase. The data clearly indicate that cytotoxic H_2O_2 was formed in a Mn porphyrin-catalyzed ascorbate consumption of oxygen [87, 101].

While the action of MnPs on transcription factors HIF-1α and AP-1 (Fig. **1**) was shown to be antioxidative [14, 21, 23, 24], the action on NF-κB was described as pro-oxidative. Coupling with SH-groups of signaling molecules (such as p50 subunit of NF-κB in nucleus) was suggested to be operative in diabetes studies [18, 82, 100]. In lymphoma studies and in the presence of H_2O_2 and glutathione (GSH), MnTE-2-PyP^{5+} was able to glutathionylate p65 subunit of NF-κB, which prevents its DNA binding, while depriving cells of GSH [26].

The effects that we are observing *in vivo* and *in vitro,* and routinely ascribing to the antioxidative action of a MnP, may instead also arise from the pro-oxidative action. In such a scenario, the increased peroxide levels could lead to the activation of cellular transcriptional activity which would result in upregulation of endogenous antioxidative defenses and a subsequent suppression of oxidative stress. Thus the antioxidative effects of MnPs could be observed, whereas the initial effect of MnPs might have been prooxidative in nature. Such events were supported by the experimental observations of Kim *et al.* [102] as well as by our *E. coli* studies, where a pro-oxidative insult (increased peroxide levels) forces *E. coli* to induce oxyR regulon and upregulate antioxidative enzymes [87]. More research is needed to clarify which action of MnPs prevails *in vivo*.

Mimicking Mitochondrial Superoxide Dismutase, MnSOD

MnTnHex-2-PyP^{5+} distributes predominantly into yeast [36], and mouse heart mitochondria relative to cytosol [Spasojevic *et al.* unpublished], where it could mimic MnSOD, the major natural antioxidant defense system (Fig. **1**). Overexpression of MnSOD has been widely shown to suppress tumor growth [38, 103,104]. In a mouse skin carcinogenesis model the effect of MnTE-2-PyP^{5+} was greater than the effect of MnSOD overexpression. While this was in part due to the possibility of administering MnP in a timely manner after cell apoptosis and before proliferation, the data strongly indicate a potential of MnP to act as MnSOD mimic in suppressing tumor growth [38, 103, 104]. The exact mechanism of MnSOD action in carcinogenesis is still not fully understood and requires future studies [38, 103, 104].

The possible actions and the advantage of the lipophilic MnTnHex-2-PyP^{5+} are summarized in Fig. (**1**). The ongoing studies are exploring the nature of the MnP antitumor activity in its own right, in particular with respect to treatment-resistant gliomas. Work is also in progress to determine if combination therapy with radiation, temozolomide and MnP can provide effective, but less toxic treatment of gliomas.

CONCLUSIONS

This is the first report on the efficacy of a redox-active metal complex in the treatment of brain tumors. MnTnHex-2-PyP^{5+} inhibited the growth of glioblastoma and medulloblastoma xenograft lines *in vivo* in both subcutaneous and intracranial tumor models, and is thus a novel and promising approach to brain tumor therapy that warrants further investigation. Its redox-based action influences cellular signaling pathways and in turn affects apoptosis and proliferation. The type of action may be pro- or antioxidative, which would depend upon the balance of cellular oxidants and antioxidants, and in particular upon the ability of the cells to remove superoxide and peroxide. It would also depend upon the tissue, cellular and subcellular accumulation of Mn porphyrin. The redox balance in tumors is known to be on the side of oxidants [91], and the resulting increased levels of reactive species appear to stimulate tumor growth. Their removal would prevent tumor cell signaling and, thus tumor growth [45]. Tumor growth suppression or induction of apoptosis could also happen *via* enhanced production of reactive species as a result of excessive oxidation of biological targets [45, 46, 49]. Therefore, both anti- and pro-oxidative actions of MnPs would result in killing of tumor cells.

Our findings justify exploring the use of MnPs in brain tumor therapy, as well as identifying the mechanism/s of action/s of these drugs. Work is also in progress to explore if the MnP treatment, when combined with radiation and chemotherapy (temozolomide), can enhance tumor growth suppression in D-245 MG brain tumor xenografts. The preliminary data indicate that MnP greatly sensitizes D-245 MG xenografts to radiation [Keir *et al.* unpublished]. New oxygen-modified Mn porphyrins are being synthesized also [105, 106]. The methoxy analogue of MnTnHex-2-PyP^{5+}, (Mn(III) *meso*-tetrakis(*N*-(6'-methoxyhexyl)pyridinium-3-yl)porphyrin, MnTMOHex-3-PyP^{5+}) has been fully characterized [105]. One other oxygen-modified analogue of superior properties have been also characterized, and the glioma study is in progress to test its therapeutic potential [106, Rajic *et al.* unpublished]. While maintaining the same antioxidant potency and the lipophilicity as MnTnHex-2-PyP^{5+}, the most prospective analogue is significantly less toxic [106]. Work is in progress on the toxicity profiles of these oxygen-modified analogues.

Acknowledgments

We are thankful to Margaret Tome for insightful discussions. This work was supported by IBH general research funds and the following NIH grants: NINDS Grant 5P50 NS20023, NCI SPORE Grant 5P50 CA108786, R01 CA40355, and NCI Merit Award R37 CA 011898. We acknowledge the help from Artak Tovmasyan and Zrinka Rajic during preparation of the manuscript.

ABBREVIATIONS

$O_2^{\cdot -}$	Superoxide
$ONOO^-$	Peroxynitrite
SOD	Superoxide dismutase
Mn	Manganese
MnSOD	Manganese superoxide dismutation
MnP	Cationic *ortho* Mn(III) substituted *N*-pyridylporphyrin
$E_{1/2}$	Metal-centered reduction potential for $Mn^{III}P^{5+}/Mn^{II}P^{4+}$ redox couple
$Mn^{III}P^{5+}$	Oxidized porphyrin with Mn in stable + 3 oxidation state
$Mn^{II}P^{4+}$	Reduced porphyrin with Mn in +2 oxidation state
NHE	Normal hydrogen electrode
P_{OW}	Partition coefficient between n-octanol and water
BBB	Blood brain barrier
GSH	Glutathione
HIF-1α	Hypoxia inducible factor 1α
AP-1	Activator protein-1
VEGF	Vascular endothelial factor
bFGF	Basic fibroblast growth factor
NF-κB	Nuclear factor κB
MnTnHex-2-PyP^{5+}	Mn(III) *meso*-tetrakis(*N*-n-hexylpyridinium-2-yl)porphyrin
MnTM-2-PyP^{5+}	Mn(III) *meso*-tetrakis(*N*-methylpyridinium-2-yl)porphyrin, AEOL10112
MnTE-2-PyP^{5+}	Mn(III) *meso*-tetrakis(*N*-ethylpyridinium-2-yl)porphyrin, AEOL10113
MnTDE-2-ImP^{5+}	Mn(III) *meso*-tetrakis(*N,N'*-diethylimidazolium-2-yl)porphyrin, AEOL10150
MnTMOHex-3-PyP^{5+}	Mn(III) *meso*-tetrakis(*N*-methoxyhexylpyridinium-3-yl)porphyrin
T-C	The difference in days between the median time required for tumors in treated (T) and control (C) animals to reach a volume five times greater than that measured at the start of treatment
ic	Intracranial
sc	Subcutaneous

CNS	Central nervous system
b.i.d.	Bis In Dies – twice daily

REFERENCES

1. Wen PY, Kesari S. Malignant gliomas in adults. N. Engl. J. Med. 2008; 359:492–507. [PubMed: 18669428]
2. Stupp R, Mason WP, van den Bent MJ, Weller M, Fisher B, Taphoorn MJ, Belanger K, Brandes AA, Marosi C, Bogdahn U, Curschmann J, Janzer RC, Ludwin SK, Gorlia T, Allgeier A, Lacombe D, Cairncross JG, Eisenhauer E, Mirimanoff RO. Radiotherapy plus concomitant and adjuvant temozolomide for glioblastoma. N. Engl. J. Med. 2005; 352:987–996. [PubMed: 15758009]
3. Lamborn KR, Yung WK, Chang SM, Wen PY, Cloughesy TF, DeAngelis LM, Robins HI, Lieberman FS, Fine HA, Fink KL, Junck L, Abrey L, Gilbert MR, Mehta M, Kuhn JG, Aldape KD, Hibberts J, Peterson PM, Prados MD. Progression-free survival: an important end point in evaluating therapy for recurrent high-grade gliomas. Neuro Oncol. 2008; 10:162–170. [PubMed: 18356283]
4. Wong ET, Hess KR, Gleason MJ, Jaeckle KA, Kyritsis AP, Prados MD, Levin VA, Yung WK. Outcomes and prognostic factors in recurrent glioma patients enrolled onto phase II clinical trials. J. Clin. Oncol. 1999; 17:2572–2578. [PubMed: 10561324]
5. Grill J, Kieffer V, Kalifa C. Measuring the neuro-cognitive side-effects of irradiation in children with brain tumors. Pediatr. Blood Cancer. 2004; 42:452–456. [PubMed: 15049019]
6. Onvani S, Etame AB, Smith CA, Rutka JT. Genetics of medulloblastoma: clues for novel therapies. Expert Rev. Neurother. 2010; 10:811–823. [PubMed: 20420498]
7. Dougherty TJ, Gomer CJ, Henderson BW, Jori G, Kessel D, Korbelik M, Moan J, Peng Q. Photodynamic therapy. J. Natl. Cancer Inst. 1998; 90:889–905. [PubMed: 9637138]
8. Nakajima S, Hayashi H, Omote Y, Yamazaki Y, Hirata S, Maeda T, Kubo Y, Takemura T, Kakiuchi Y, Shindo Y. The tumour-localizing properties of porphyrin derivatives. J. Photochem. Photobiol. B. 1990; 7:189–198. [PubMed: 2128323]
9. Nakajima S, Sakata I, Omote Y, Yamazaki K, Maeda T, Kubo Y, Samejima N, Takemura T, Shindo Y, Yamauchi H. Detection and quantitative estimation of metalloporphyrins *in vivo*. J. Photochem. Photobiol. B. 1991; 8:409–417. [PubMed: 1904489]
10. Nakajima S, Yamauchi H, Sakata I, Hayashi H, Yamazaki K, Maeda T, Kubo Y, Samejima N, Takemura T. ^{111}In-labeled Mn-metalloporphyrin for tumor imaging. Nucl. Med. Biol. 1993; 20:231–237. [PubMed: 8448578]
11. Nakajima S, Shigemi N, Murakami N, Aburano T, Sakata I, Maruyama I, Inoue M, Takemura T. Therapeutic and imaging capacity of tumor-localizing radiosensitive Mn-porphyrin on SCCVII tumor-bearing C3H/He mice. Anticancer Drugs. 1997; 8:386–390. [PubMed: 9180393]
12. Nakajima S, Sakata I, Hirano T, Takemura T. Therapeutic effect of interstitial photodynamic therapy using ATX-S10(Na) and a diode laser on radio-resistant SCCVII tumors of C3H/He mice. Anticancer Drugs. 1998; 9:539–543. [PubMed: 9877242]
13. Nakajima S, Fujii T, Murakami N, Aburano T, Sakata I, Nakae Y, Takemura T. Therapeutic and imaging capacity of tumor-localizing radiosensitive Mn-porphyrin KADT-F10 for SCCVII tumors in C3H /He mice. Cancer Lett. 2002; 181:173–178. [PubMed: 12175532]
14. Benov L, Craik J, Batinic-Haberle I. Protein damage by photo-activated Zn(II) N-alkylpyridylporphyrins. Amino Acids. 2010
15. Arambula JF, Preihs C, Brothwick D, Magda D, Jonathan L, Sessler JL. Texaphyrins: Tumor Localizing Redox Active Expanded Porphyrins. Submitted to Anticancer Agents Med. Chem.
16. Batinic-Haberle I, Reboucas JS, Spasojevic I. Superoxide Dismutase Mimics: Chemistry, Pharmacology, and Therapeutic Potential. Antioxid. Redox Signal. 2010
17. Batinic-Haberle, I.; Reboucas, JS.; Benov, L.; Spasojevic, I. Chemistry, biology and medical effects of water-soluble metalloporphyrins. In: Kadish, KM.; Smith, KM.; Guilard, R., editors. Handbook of Porphyrin Science. Vol. Vol 11. World Scientific; 2010. (in press).

18. Batinic-Haberle I, Spasojevic I, Tse HM, Tovmasyan A, Rajic Z, St. Clair DK, Vujaskovic Z, Dewhirst MW, Piganelli JD. Design of Mn porhyrins for treating oxidative stress injuries and their redox-based regulation of cellular transcriptional activities. Amino Acids. 2010
19. Rabbani ZN, Salahuddin FK, Yarmolenko P, Batinic-Haberle I, Thrasher BA, Gauter-Fleckenstein B, Dewhirst MW, Anscher MS, Vujaskovic Z. Low molecular weight catalytic metalloporphyrin antioxidant AEOL 10150 protects lungs from fractionated radiation. Free Radic. Res. 2007; 41:1273–1282. [PubMed: 17957541]
20. Gauter-Fleckenstein B, Fleckenstein K, Owzar K, Jiang C, Batinic-Haberle I, Vujaskovic Z. Comparison of two Mn porphyrin-based mimics of superoxide dismutase in pulmonary radioprotection. Free Radic. Biol. Med. 2008; 44:982–989. [PubMed: 18082148]
21. Rabbani ZN, Spasojevic I, Zhang X, Moeller BJ, Haberle S, Vasquez-Vivar J, Dewhirst MW, Vujaskovic Z, Batinic-Haberle I. Antiangiogenic action of redox-modulating Mn(III) meso-tetrakis(*N*-ethylpyridinium-2-yl)porphyrin, MnTE-2-PyP^{5+}, *via* suppression of oxidative stress in a mouse model of breast tumor. Free Radic. Biol. Med. 2009; 47:992–1004. [PubMed: 19591920]
22. Moeller BJ, Batinic-Haberle I, Spasojevic I, Rabbani ZN, Anscher MS, Vujaskovic Z, Dewhirst MW. A manganese porphyrin superoxide dismutase mimetic enhances tumor radioresponsiveness. Int. J. Radiat. Oncol. Biol. Phys. 2005; 63:545–552. [PubMed: 16168847]
23. Moeller BJ, Cao Y, Li CY, Dewhirst MW. Radiation activates HIF-1 to regulate vascular radiosensitivity in tumors: role of oxygenation, free radicals and stress granules. Cancer Cell. 2004; 5:429–441. [PubMed: 15144951]
24. Zhao Y, Chaiswing L, Oberley TD, Batinic-Haberle I, St. Clair W, Epstein CJ, St, Clair D. A mechanism-based antioxidant approach for the reduction of skin carcinogenesis. Cancer Res. 2005; 65:1401–1405. [PubMed: 15735027]
25. Jaramillo MC, Frye JB, Crapo JD, Briehl MM, Tome ME. Increased manganese superoxide dismutase expression or treatment with manganese porphyrin potentiates dexamethasone-induced apoptosis in lymphoma cells. Cancer Res. 2009; 69:5450–5457. [PubMed: 19549914]
26. Jaramillo MC, Briehl MM, Tome ME. Manganese porphyrin glutathionylates the p65 subunit of NF-κB to potentiate glucocorticoid-induced apoptosis in lymphoma. Free Radic. Biol. Med. 2010; 49:S63.
27. Makinde AY, Luo-Owen X, Rizvi A, Crapo JD, Pearlstein RD, Slater JM, Gridley DS. Effect of a metalloporphyrin antioxidant (MnTE-2-PyP) on the response of a mouse prostate cancer model to radiation. Anticancer Res. 2009; 29:107–118. [PubMed: 19331139]
28. Kos I, Rebouças JS, DeFreitas-Silva G, Salvemini D, Vujaskovic Z, Dewhirst MW, Spasojevic I, Batinic-Haberle I. The effect of lipophilicity of porphyrin-based antioxidants. Comparison of *ortho* and *meta* isomers of Mn(III) *N*-alkylpyridylporphyrins. Free Radic. Biol. Med. 2009; 47:72–78. [PubMed: 19361553]
29. Sheng H, Tse HM, Jung JY, Zhang Z, Spasojevic I, Piganelli JD, Batinic-Haberle I, Warner D. Neuroprotective efficacy from a lipophilic redox-modulating Mn porphyrin: rodent models of ischemic stroke and subarachnoid hemorrhage. J. Pharmacol. Exp. Ther. 2011 (under revision).
30. Doyle T, Bryant L, Batinic-Haberle I, Little J, Cuzzocrea S, Masini E, Spasojevic I, Salvemini D. Supraspinal inactivation of mitochondrial superoxide dismutase is a source of peroxynitrite in the development of morphine antinociceptive tolerance. Neuroscience. 2009; 164:702–710. [PubMed: 19607887]
31. Spasojevic I, Kos I, Benov LT, Rajic Z, Fels D, Dedeugd C, Ye X, Vujaskovic Z, Reboucas JS, Leong KW, Dewhirst MW, Batinic-Haberle I. Bioavailability of metalloporphyrin-based SOD mimics is greatly influenced by a single charge residing on a Mn site. Free Radic. Res. 2010; 45:188–200. [PubMed: 20942564]
32. Pollard JM, Rebouças JS, Durazo A, Kos I, Fike F, Panni M, Gralla EB, Valentine JS, Batinic-Haberle I, Gatti RA. Radioprotective effects of manganese-containing superoxide dismutase mimics on ataxia telangiectasia cells. Free Radic. Biol. Med. 2009; 47:250–260. [PubMed: 19389472]
33. Yu L, Drobyshevsky A, Derricka M, Luo T, Batinic-Haberle I, Tan S. Efferct of Mn porphyrins and antioxidants on MRI predictors and behavior in an animal model of cerebral palsy. Free Radic. Biol. Med. 2010; 49:S159.

34. Murphy MP, Smith RAJ. Targeting antioxidants to mitochondria by conjugation to lipophilic cations. Annu. Rev. Pharmacol. Toxicol. 2007; 47:629–656. [PubMed: 17014364]
35. Murphy MP. Targeting lipophilic cations to mitochondria. Biochim. Biophys. Acta. 2008; 177:1028–1031. [PubMed: 18439417]
36. Spasojevic I, Li AM, Tovmasyan A, Rajic Z, Salvemini D, St. Clair D, Valentine JS, Vujaskovic Z, Gralla EB, Batinic-Haberle I. Accumulation of porphyrin-based SOD mimics in mitochondria is proportional to their lipophilicity. *S. cerevisiae* study of *ortho* Mn(III) *N*-alkylpyridylporphyrins. Free Radic. Biol. Med. 2010; 49:S199.
37. Spasojevic I, Yumin C, Noel T, Yu I, Pole MP, Zhang L, Zhao Y, St. Clair DK, Batinic-Haberle I. Mn porphyrin-based SOD mimic, MnTE-2-PyP^{5+} targets mouse heart mitochondria. Free Radic. Biol. Med. 2007; 42:1193–1200. [PubMed: 17382200]
38. Miriyala S, Holley AK, St Clair DK. MnSOD - Signals of distinction (SOD). Submitted to Anticancer Agents Med. Chem.
39. Friedman HS, Colvin OM, Skapek SX, Ludeman SM, Elion GB, Schold SC Jr, Jacobsen PF, Muhlbaier LH, Bigner DD. Experimental chemotherapy of human medulloblastoma cell lines and transplantable xenografts with bifunctional alkylating agents. Cancer Res. 1988; 48:4189–4195. [PubMed: 3390813]
40. Sathornsumetee S, Hjelmeland AB, Keir ST, McLendon RE, Batt D, Ramsey T, Yusuff N, Rasheed BK, Kieran MW, Laforme A, Bigner DD, Friedman HS, Rich JN. AAL881, a novel small molecule inhibitor of RAF and vascular endothelial growth factor receptor activities, blocks the growth of malignant glioma. Cancer Res. 2006; 66:8722–8730. [PubMed: 16951188]
41. Gamez I, Ryan RP, Keir ST. Corticorelin Acetate, a Synthetic Corticotropin-releasing Factor with Preclinical Antitumor Activity, alone and with Bevacizumab, against Human Brain Tumor Models. Anticancer Res. 2010; 30:5037–5042. [PubMed: 21187487]
42. Friedman HS, Schold SC Jr, Bigner DD. Chemotherapy of Subcutaneous and Intracranial Human Medulloblastoma Xenografts in Athymic Nude Mice. Cancer Res. 1986; 46:224–228. [PubMed: 2415246]
43. Pollack IF, Bredel M, Erff M, Hamilton AD, Sebti SM. Inhibition of Ras and related guanosine triphosphate-dependent proteins as a therapeutic strategy for blocking malignant glioma growth: II--preclinical studies in a nude mouse model. Neurosurgery. 1999; 45:1208–1214. discussion 1214–1215. [PubMed: 10549939]
44. Gehan EA. A Generalized Wilcoxon Test for Comparing Arbitrarily Singly-Censored Samples. Biometrika. 1965; 52:203–223. [PubMed: 14341275]
45. Liou GY, Storz P. Reactive oxygen species in cancer. Free Radic. Res. 2010; 44:479–496. [PubMed: 20370557]
46. Storz P. Reactive oxygen species in tumor progression. Front Biosci. 2005; 10:1881–1896. [PubMed: 15769673]
47. Halliwell, B.; Gutteridge, J. Free radicals in biology and medicine. 4th edition ed. New York: Oxford Press; 2007.
48. Ridnour LA, Oberley TD, Oberley LW. Tumor suppressive effects of MnSOD overexpression may involve imbalance in peroxide generation versus peroxide removal. Antioxid. Redox Signal. 2004; 6:501–512. [PubMed: 15130277]
49. Hernandez-Garcia D, Wood CD, Castro-Obregon S, Covarrubias L. Reactive oxygen species: a radical role in development? Free Radic. Biol. Med. 2010; 49:130–143. [PubMed: 20353819]
50. Chan SC, Hui L, Chen HM. Enhancement of the cytolytic effect of anti-bacterial peptide cecropin by the microvilli of cancer cells. Anticancer Res. 1998; 18:4467–4474. [PubMed: 9891511]
51. Zwaal RF, Schroit AJ. Pathophysiologic implications of membrane phospholipid asymmetry in blood cells. Blood. 1997; 89:1121–1132. [PubMed: 9028933]
52. Hoskin DW, Ramamoorthy A. Studies on anticancer activities of antimicrobial peptides. Biochim. Biophys. Acta. 2008; 1778:357–375. [PubMed: 18078805]
53. Schweizer F. Cationic amphiphilic peptides with cancer-selective toxicity. Eur. J. Pharmacol. 2009; 625:190–194. [PubMed: 19835863]

54. Kornguth SE, Kalianke T, Robins HI, Cohen JD, Turski P. Preferential binding of radiolabeled poly-L-lysine to C6 and U87 MG glioblastomas compared to endothelial cells *in vitro*. Cancer Res. 1989; 49:6390–6395. [PubMed: 2804985]
55. Jensen TJ, Vicente MGH, Luguya R, Norton J, Fronczek FR, Smith KM. Effect of overall charge and charge distribution on cellular uptake, distribution and phototoxicity of cationic porphyrins in Hep2 cells. J. Photochem. Photobiol. B: Biol. 2010; 100:100–111.
56. Merchant TE, Pollack IF, Loeffler JS. Brain tumors across the age spectrum: biology, therapy, and late effects. Semin. Radiat. Oncol. 2010; 20:58–66. [PubMed: 19959032]
57. Padovani L, André N, Carrie C, Muracciole X. Childhood and adult medulloblastoma: what difference? Cancer Radiother. 2009; 13:530–535. [PubMed: 19713143]
58. Prados MD, Russo C. Chemotherapy of brain tumors. Semin. Surg. Oncol. 1998; 14:88–95. [PubMed: 9407635]
59. Karajannis M, Allen JC, Newcomb EW. Treatment of pediatric brain tumors. J. Cell Physiol. 2008; 217:584–589. [PubMed: 18651562]
60. Fan QW, Weiss WA. Targeting the RTK-PI3K-mTOR axis in malignant glioma: overcoming resistance. Curr. Top. Microbiol. Immunol. 2010; 347:279–296. [PubMed: 20535652]
61. Quant EC, Wen PY. Novel medical therapeutics in glioblastomas, including targeted molecular therapies, current and future clinical trials. Neuroimaging Clin. N. Am. 2010; 20:425–448. [PubMed: 20708556]
62. Gogvadze V, Orrenius S, Zhivotovsky B. Mitochondria as targets for chemotherapy. Apoptosis. 2009; 14:624–640. [PubMed: 19205885]
63. Kanu OO, Mehta A, Di C, Lin N, Bortoff K, Bigner DD, Yan H, Adamson DC. Glioblastoma multiforme: a review of therapeutic targets. Expert Opin. Ther. Targets. 2009; 13:701–718. [PubMed: 19409033]
64. Gauter-Fleckenstein B, Fleckestein K, Owzar K, Jiang C, Reboucas JS, Batinic-Haberle I, Vujaskovic Z. Early and late administration of antioxidant mimic MnTE-2-PyP^{5+} in mitigation and treatment of radiation-induced lung damage. Free Radic. Biol. Med. 2010; 48:1034–1043. [PubMed: 20096348]
65. Li H, Wang Y, Senthil K, Pazhanisamy SK, Shao L, Batinic-Haberle I, Meng A, Zhou D. Treatment with Mn(III) meso-tetrakis(N-ethylpyridinium-2-yl)porphyrin (MnTE-2-PyP^{5+}) mitigates total body irradiation-induced long-term bone marrow suppression. Free. Radic. Biol. Med. 2010 (under revision).
66. Pearlstein RD, Higuchi Y, Moldovan M, Johnson K, Fukuda S, Gridley DS, Crapo JD, Warner DS, Slater JM. Metalloporphyrin antioxidants ameliorate normal tissue radiation damage in rat brain. Int. J. Radiat. Biol. 2010; 86:145–163. [PubMed: 20148700]
67. Makinde AY, Rizvi A, Crapo JD, Pearlstein RD, Slater JM, Gridley DS. A metalloporphyrin antioxidant alters cytokine responses after irradiation in a prostate tumor model. Radiat. Res. 2010; 173:441–452. [PubMed: 20334516]
68. Pazhanisamy SK, Li H, Batinic-Haberle I, Zhou D. NADPH oxidase inhibition attenuates total body-irrradiation-induced hematopoietic genomic instability. Mutagenesis. 2010 (in press).
69. Mao XW, Crapo JD, Mekonnen T, Lindsey N, Martinez P, Gridley DS, Slater JM. Radioprotective effect of a metalloporphyrin compound in rat eye model. Curr. Eye Res. 2009; 34:62–72. [PubMed: 19172472]
70. Lee JH, Park JW. A manganese porphyrin complex is a novel radiation protector. Free Radic. Biol. Med. 2004; 37:272–283. [PubMed: 15203198]
71. Nebert DW, Mason HS. An Electron Spin Resonance Study of Neoplasms. Cancer Res. 1963; 23:833–840. [PubMed: 14085278]
72. Reuter S, Gupta SC, Chaturvedi MM, Aggrawal BB. Oxidative stress, inflammation, and cancer: how are they linked? Free Radic. Biol. Med. 2010; 49:1603–1616. [PubMed: 20840865]
73. Grek CL, Tew KD. Redox metabolism and malignancy. Curr. Opin. Pharmacol. 2010; 10:362–368. [PubMed: 20627682]
74. Bell EL, Klimova TA, Eisenbart J, Moraes CT, Murphy MP, Budinger GR, Chandel NS. The Qo site of the mitochondrial complex III is required for the transduction of hypoxic signaling *via* reactive oxygen species production. J. Cell Biol. 2007; 177:1029–1036. [PubMed: 17562787]

75. Chandel NS, McClintock DS, Feliciano CE, Wood TM, Melendez JA, Rodriguez AM, Schumacker PT. Reactive oxygen species generated at mitochondrial complex III stabilize hypoxia-inducible factor-1alpha during hypoxia: a mechanism of O_2 sensing. J. Bol. Chem. 2000; 275:25130–25138.
76. Dewhirst MW. Relationships between cycling hypoxia, HIF-1, angiogenesis and oxidative stress. Rad. Res. 2009; 172:653–665.
77. Dewhirst MW, Cao Y, Moeller B. Cycling hypoxia and free radicals regulate angiogenesis and radiotherapy response. Nat. Rev. 2008; 8:425–437.
78. Bristow RG, Hill RP. Hypoxia and metabolism. Hypoxia, DNA repair and genetic instability. Nat. Rev. 2008; 8:180–192.
79. Bulut AS, Erden E, Sak SD, Doruk H, Kursun N, Dincol D. Significance of inducible nitric oxide synthase expression in benign and malignant breast epithelium: an immunohistochemical study of 151 cases. Virchows Arch. 2005; 447:24–30. [PubMed: 15947943]
80. Nakamura Y, Yasuoka H, Tsujimoto M, Yoshidome K, Nakahara M, Nakao K, Nakamura M, Kakudo K. Nitric oxide in breast cancer: induction of vascular endothelial growth factor-C and correlation with metastasis and poor prognosis. Clin. Cancer Res. 2006; 12:1201–1207. [PubMed: 16489074]
81. Szabó C, Ischiropoulos H, Radi R. Peroxynitrite: biochemistry, pathophysiology and development of therapeutics. Nat. Rev. Drug Discov. 2007; 6:662–680. [PubMed: 17667957]
82. Tse HM, Milton MJ, Piganelli JD. Mechanistic analysis of the immunomodulatory effects of a catalytic antioxidant on antigen-presenting cells: implication for their use in targeting oxidation-reduction reactions in innate immunity. Free Radic. Biol. Med. 2004; 36:233–247. [PubMed: 14744635]
83. Batinic-Haberle I, Spasojević I, Stevens RD, Hambright P, Neta P, Okado-Matsumoto A, Fridovich I. New class of potent catalysts of $O_2^{\cdot -}$ dismutation. Mn(III) methoxyethylpyridyl- and methoxyethylimidazolylporphyrins. J. Chem. Soc. Dalton Trans. 2004; 11:1696–1702.
84. Verrax J, Curi Pedrosa R, Beck R, Dejeans N, Taper H, Buc Calderon P. In situ modulation of oxidative stress: a novel and efficient strategy to kill cancer cells. Curr. Med. Chem. 2009; 16:1821–1830. [PubMed: 19442148]
85. Harrison FR, May JM. Vitamin C function in the brain: vital role of the ascorbate transporter SVCT2. Free Radic. Biol. Med. 2009; 46:719–730. [PubMed: 19162177]
86. Verrax J, Calderon PB. The controversial place of vitamin C in cancer treatment. Biochem. Pharmacol. 2008; 76:1644–1652. [PubMed: 18938145]
87. Batinic-Haberle I, Rajic Z, Benov L. A combination of two antioxidants produces a prooxidative effect forcing *Escherichia coli* to adapt *via* induction of *oxyR* regulon. Anticancer Agents Med. Chem. submitted.
88. Williams NH, Yandell JK. Outer-sphere Electron-Transfer Reactions of Ascorbate Anions. Aust. J. Chem. 1982; 35:1133–1144.
89. Imlay JA. Cellular defenses against superoxide and hydrogen peroxide. Annu. Rev. Biochem. 2008; 77:755–776. [PubMed: 18173371]
90. Jang S, Imlay JA. Micromolar intracellular hydrogen peroxide disrupts metabolism by damaging iron-sulfur enzymes. J. Biol. Chem. 2007; 282:929–937. [PubMed: 17102132]
91. Shan W, Zhong W, Zhao R, Oberley TD. Thioredoxin 1 as a subcellular biomarker of redox imbalance in human prostate cancer progression. Free Rad. Biol. Med. 2010; 49:2078–2087. [PubMed: 20955789]
92. Sessler JL, Miller RA. Texaphyrins: new drugs with diverse clinical applications in radiation and photodynamic therapy. Biochem. Pharmacol. 2000; 59:733–739. [PubMed: 10718331]
93. Viani GA, Manta GB, Fonseca EC, De Fendi LI, Afonso SL, Stefano EJ. Whole brain radiotherapy with radiosensitizer for brain metastases. J. Exp. Clin. Cancer Res. 2009; 28:1. [PubMed: 19126230]
94. Crow JP, Calinasan NY, Chen J, Hill JL, Beal MF. Manganese porphyrin given at symptom onset markedly extends survival of ALS mice. Ann. Neurol. 2005; 58:258–265. [PubMed: 16049935]

95. Ye X, Fels D, Dedeugd C, Dewhirst MW, Leong K, Batinic-Haberle I. The *in vitro* cytotoxic effects of Mn(III) alkylpyridylporphyrin/ascorbate system on four tumor cell lines. Free Radic. Biol. Med. 2009; 47:S136.

96. Chen Q, Espey MG, Sun AY, Pooput C, Kirk KL, Krishna MC, Khosh DB, Drisko J, Levine M. Pharmacologic doses of ascorbate act as a pro-oxidant and desrease growth of aggressive tumor xenografts in mice. Proc. Natl. Acad. Sci. U.S.A. 2008; 105:11105–11109. [PubMed: 18678913]

97. Verrax J, Beck R, Dejeans N, Glorieux C, Sid B, Curi Pedrosa R, Benites J, Vásquez D, Valderrama JA, Buc Calderon P. Redox-active quinones and ascorbate: an innovative cancer therapy that exploits the vulnerability of cancer cells to oxidative stress. Anticancer Agents Med. Chem. 2011 (this Issue, submitted).

98. Ohno S, Ohno Y, Suzuki N, Soma G, Inoue M. High-dose vitamin C (ascorbic acid) therapy in the treatment of patients with advanced cancer. Anticancer Res. 2009; 29:809–815. [PubMed: 19414313]

99. Chen Q, Espey MG, Sun AY, Lee J-H, Krishna MC, Shacter E, Choyke PL, Pooput C, Kirk KL, Buettner GR, Levine M. Ascorbate in pharmacologic concentrations selectively generates ascorbate radical and hydrogen peroxide in extracellular fluid *in vivo*. Proc. Natl. Acad. Sci. USA. 2007; 104:8749–8754. [PubMed: 17502596]

100. Piganelli JD, Flores SC, Cruz C, Koepp J, Young R, Bradley B, Kachadourian R, Batinić-Haberle I, Haskins K. A Metalloporphyrin Superoxide Dismutase Mimetic (SOD Mimetic) Inhibits Autoimune Diabetes. Diabetes. 2002; 51:347–355. [PubMed: 11812741]

101. Rajic Z, Benov L, Kos I, Tovmasyan A, Batinic-Haberle I. Cationic Mn porphyrins change their action from anti- to prooxidative in the presence of cellular reductants. Relevance to understanding the beneficial therapeutic effects of SOD mimics in mammalian systems. Free Radic. Biol. Med. 2010; 49:S194.

102. Kim A, Joseph S, Khan A, Epstein CJ, Sobel R, Huang T-T. Enhanced expression of mitochondrial superoxide dismutase leads to prolonged *in vivo* cell cycle progression and up-regulation of mitochondrial thioredoxin. Free Radic. Biol. Med. 2010; 48:1501–1512. [PubMed: 20188820]

103. Hempel N, Carrico PM, Melendez JA. Manganese superoxide dismutase (Sod2) and redox-control of signaling events that drive metastasis. Submitted to Anticancer Agents Med. Chem. 2011 This Issue.

104. MacMillan-Crow LA, Crow J. Does More MnSOD Mean More Hydrogen Peroxide? Anticancer Agents Med. Chem. 2011 (this Issue, in press).

105. Tovmasyan A, Rajic Z, Spasojevic I, Reboucas JS, Chen X, Sheng H, Warner DS, Benov L, Batinic-Haberle I. Methoxy-derivatization of alkyl chains increases the efficacy of cationic Mn porphyrins. Synthesis, characterization, SOD-like activity, and SOD-deficient E. coli study of meta Mn(III) N-methoxyalkylpyridylporphyrins. Dalton Trans. 2011

106. Batinic-Haberle I, Rajic Z, Tovmasyan A, Dewhirst M, Spasojevic I. Diverse functions of cationic Mn(III) substituted *N*-pyridylporphyrins, known as SOD mimics. Free Radic. Biol. Med. (under revision).

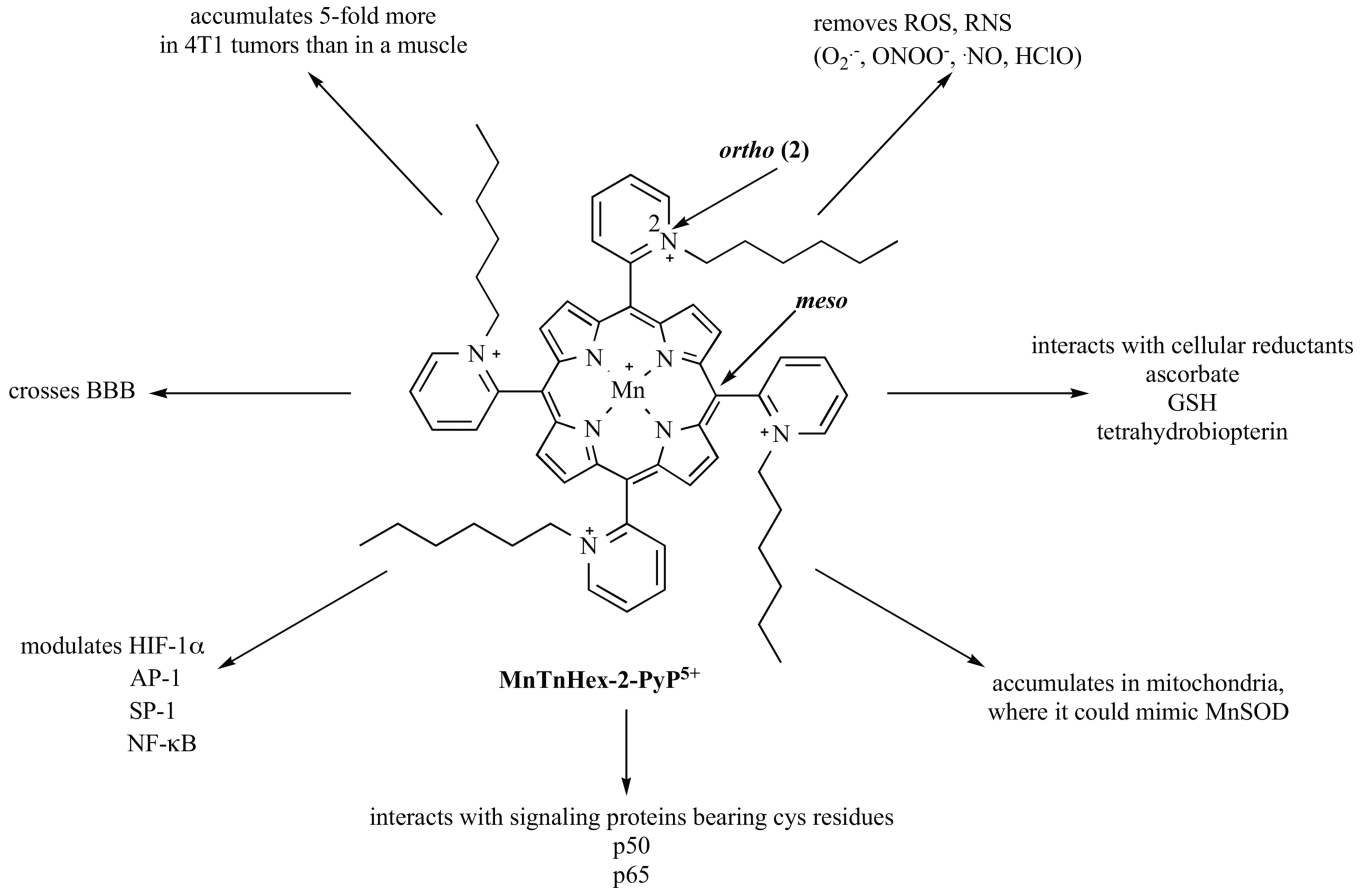

Fig. (1).

The structure, *in vivo* actions and the beneficial properties of the lipophilic *ortho* isomeric Mn(III) *meso*-tetrakis(*N*-n-hexylpyridinium-2-yl)porphyrin, MnTnHex-2-PyP^{5+}. MnTnHex-2-PyP^{5+} accumulates in yeast (>90%) and mouse heart mitochondria (>80%), and in 4T1 breast tumor, and crosses the blood brain barrier. It is among the most potent SOD mimics and peroxynitrite scavengers (Table **1**). Its ethyl analogue, MnTE-2-PyP^{5+} reportedly inhibits activation of several major transcription factors either *via* removing signaling species or *via* direct interactions with these proteins. Based on the nearly identical redox properties of those two Mn porphyrins (Table **1**) and their equal overall charge, the same ability to inhibit transcription factors was found with NF-κB and HIF-1α for MnTnHex-2-PyP^{5+} and was thus presumed operative for AP-1, and SP-1 also. Its interactions with cellular reductants may result in anti- and pro-oxidative actions (see Discussion). Interactions with NF-κB were discussed as being pro-oxidative, affecting the p50 and p65 subunits of NF-κB (see Discussion). Glutathionylation of p65 by MnTE-2-PyP^{5+} was shown to prevent DNA binding (see Discussion). Thus far, the interactions of MnPs with HIF-1α and AP-1 were described as antioxidative in nature.

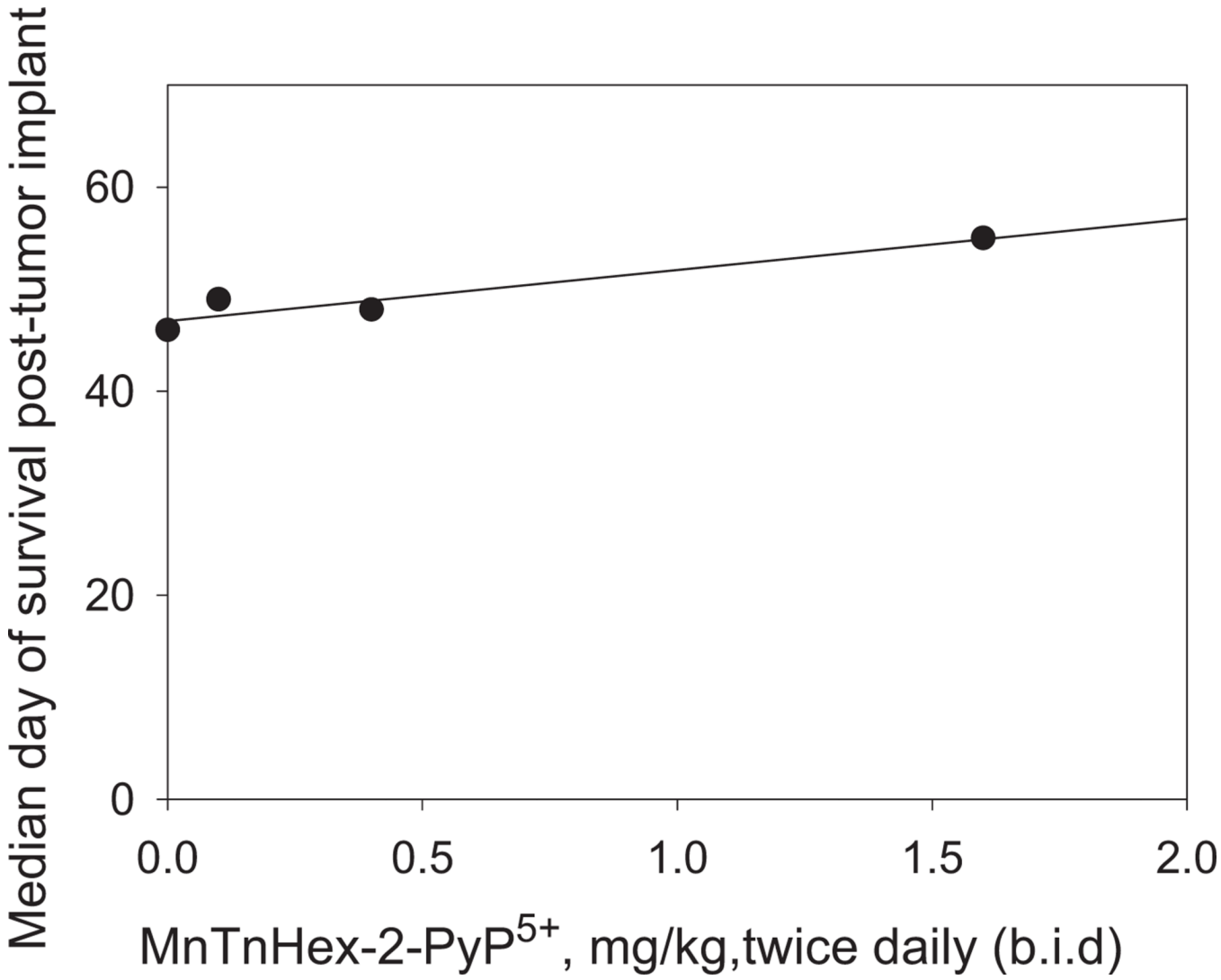

Fig. (2).
Toxicity evaluation of MnP treatment in mice bearing intracranial D-245 MG xenografts. Median day of survival post-tumor implant is plotted *vs* the dose of MnTnHex-2-PyP^{5+} in mg/kg given sc b.i.d.. Treatment started 3 days post tumor implant.

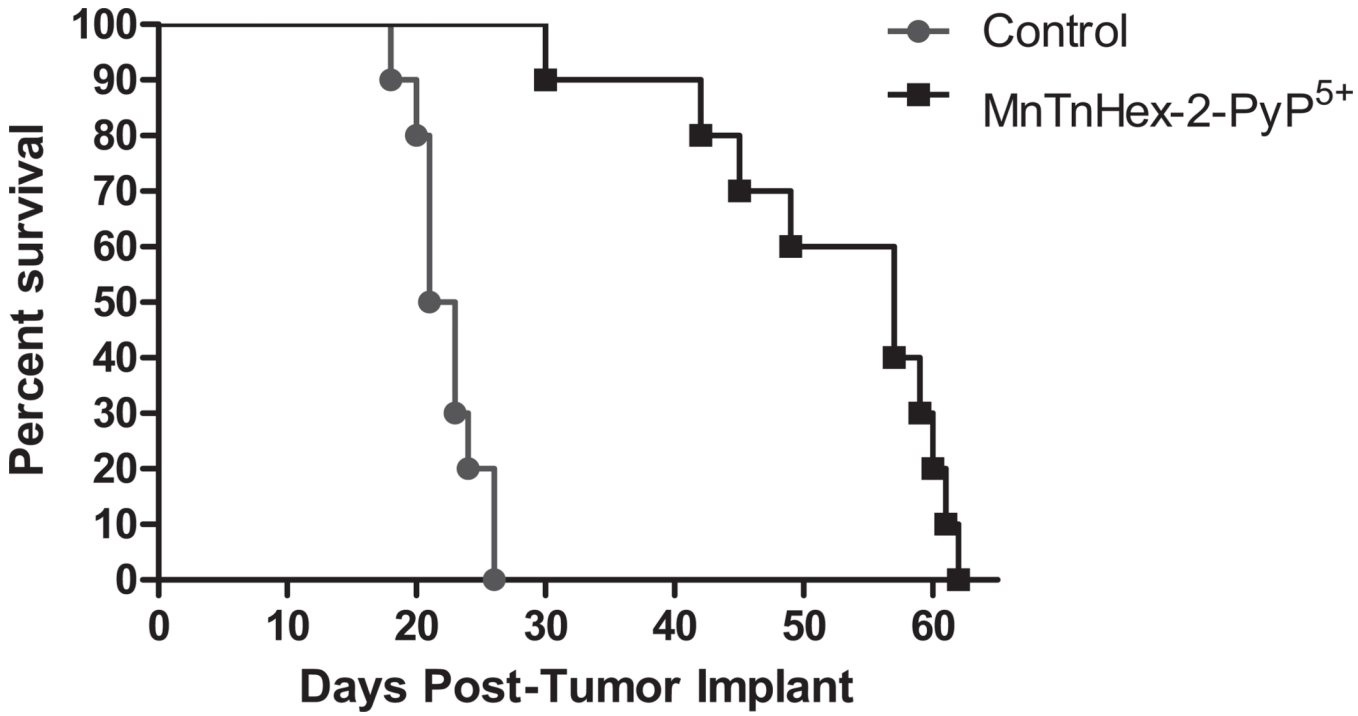

Fig. (3).

Survival Curves: Effect of MnTnHex-2-PyP^{5+} treatment on the survival of mice bearing intracranial human pediatric medulloblastoma D-341 MED xenografts. MnTnHex-2-PyP^{5+} was given sc at a dose of 1.6 mg/kg b.i.d. throughout the duration of experiment.

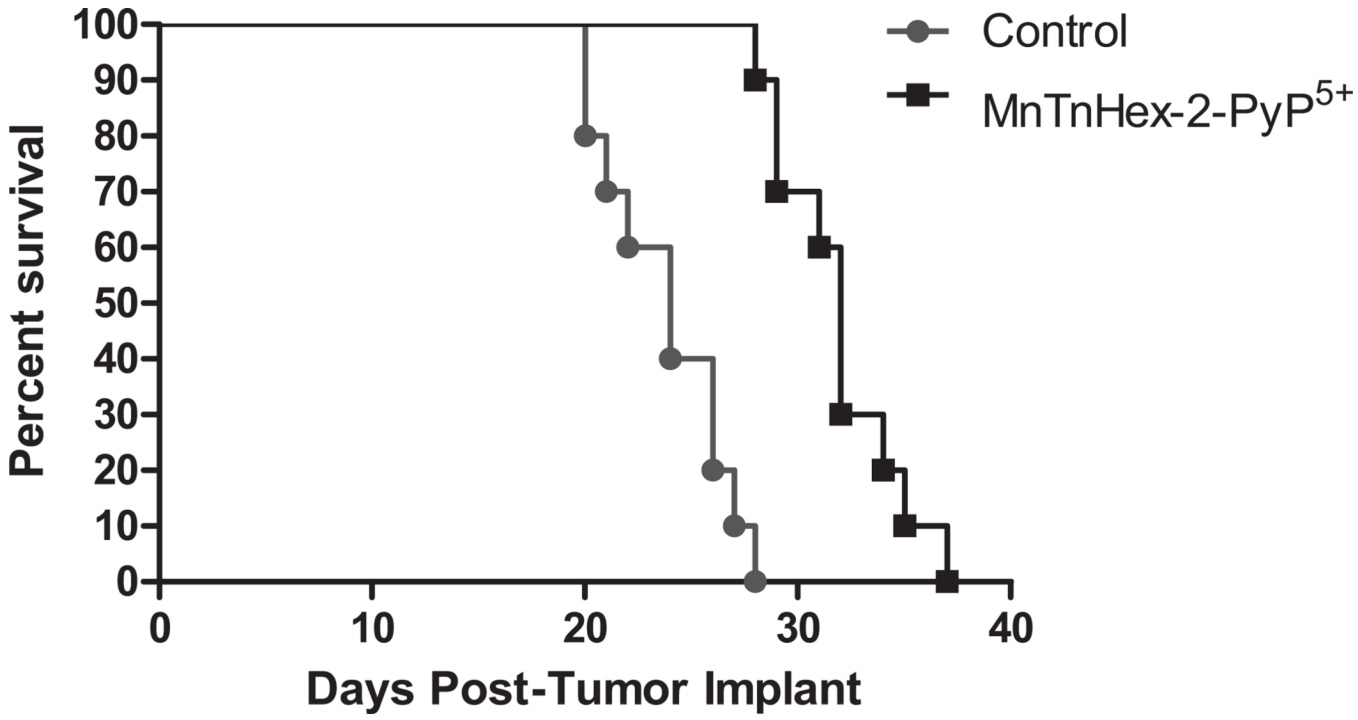

Fig. (4).

Survival curves: Effect of MnTnHex-2-PyP^{5+} treatment on the survival of mice bearing intracranial human glioblastoma multiforme D-256 MG xenografts. MnTnHex-2-PyP^{5+} was given sc at a dose of 1.6 mg/kg b.i.d. throughout the duration of experiment.

Table 1

Metal-Centered Reduction Potential, $E_{1/2}$ for $Mn^{III}P^{5+}/Mn^{II}P^{4+}$ Redox Couple, and the Rate Constants for the Dismutation of $O_2^{\cdot -}$ and Reduction of $ONOO^-$ by MnTnHex-2-PyP^{5+}. Also the partition of the compound between n-octanol and water, P_{OW} was given as a measure of its lipophilicity. The data for another hydrophilic but equally potent compound, MnTE-2-PyP^{5+} {*ortho* isomer, Mn(III) *meso*-tetrakis(*N*-ethylpyridinium-2-yl)porphyrin, AEOL10113}, as well as for SOD enzymes were given here for a comparison[a]

Compound	$E_{1/2}$, mV *vs* NHE[b]	log $k_{cat}(O_2^{\cdot -})$[c]	log $k_{red}(ONOO^-)$[d]	log P_{OW}[e]
MnTnHex-2-PyP^{5+}	+314	7.48	7.11	−2.76
MnTE-2-PyP^{5+}	+228	7.76	7.53	−6.89
SODs	~+300	8.84–9.30	3.97	

[a] The details are given in references 16 and 17.

[b] $E_{1/2}$ was determined in 0.05 M phosphate buffer (pH 7.8, 0.1 M NaCl);

[c] k_{cat} was determined by cytochrome *c* assay in 0.05 M phosphate buffer (pH 7.8, at 25±1 °C);

[d] $k_{red}(ONOO^-)$ was determined in 0.05 M phosphate buffer, 37 ± 0.1 °C;

[e] P_{OW} describes a partition of the compound between n-octanol and water.

Table 2

The Effect of MnTnHex-2-PyP^{5+} Treatment on the Growth of Subcutaneous Human Brain Tumor Xenografts in Mice. MnTnHex-2-PyP^{5+} was given sc at a dose of 1.6 mg/kg b.i.d. throughout the duration of experiment. T-C, is defined as the difference in days between the median time required for tumors in treated (T) and control (C) animals to reach a volume five times greater than that measured at the start of treatment

Xenograft	Histology	Adult/Pediatric	*In Vivo* Results		
			T-C (days)	P Value	Regressions
D-54 MG	Glioblastoma multiforme	Adult	3	≤0.345	0/10
D-245 MG	Glioblastoma multiforme	Adult	11	≤0.001	1/10
D-256 MG	Glioblastoma multiforme	Adult	4.3	≤0.001	0/10
D-341 MED	Medulloblastoma	Pediatric	34	≤0.001	10/10
D-456 MG	Glioblastoma multiforme	Pediatric	21.3	≤0.001	10/10

Table 3

The Effect of MnTnHex-2-PyP^{5+} Treatment on the Survival Of Mice Bearing Intracranial Human Brain Tumor Xenografts. MnTnHex-2-PyP^{5+} was given sc at a dose of 1.6 mg/kg b.i.d. throughout the duration of experiment

Xenograft	Histology	Adult/Pediatric	*In Vivo* Results	
			% Increase in Survival	P Value
D-54 MG	Glioblastoma multiforme	Adult	0%	NS
D-245 MG	Glioblastoma multiforme	Adult	20%	<0.111
D-256 MG	Glioblastoma multiforme	Adult	33%	≤0.001
D-341 MED	Medulloblastoma	Pediatric	171%	≤0.001